

MECHANICS OF DEBRIS FLOWS AND DEBRIS-LADEN FLASH FLOODS

By Richard M. Iverson, Hydrologist, USGS, Vancouver, Washington;
Roger P. Denlinger, Geophysicist, USGS, Vancouver, Washington

Abstract: A new mathematical model developed to predict behavior of debris flows and avalanches also holds promise for predicting behavior of debris-laden flash floods. The model assumes that debris flows behave as mixtures of interacting Newtonian fluids and Coulomb solids. Solid and fluid constituents obey three-dimensional mass and momentum balances, which are summed and depth-integrated to yield equations that describe shallow flows of the mixture as a whole. An important distinction between these mixture equations and standard shallow-water equations results from strong variation of flow resistance due to interacting solid and fluid forces. Partitioning of flow resistance between solid and fluid components depends on fluid pressure, which evolves as flow evolves. If fluid pressure supports the total weight of the flowing mass, all resistance results from hydrodynamic forces, and the equations reduce to the conventional shallow-water form. If fluid pressure supports none of the weight of the flowing mass, all flow resistance results from Coulomb friction between interacting solids, and the equations describe motion of granular avalanches. A combination of solid and fluid resistance typifies debris flows and debris-laden flash floods. In these flows solid resistance commonly is concentrated at the fronts of advancing bores that may be heavily freighted with rocks and woody debris. Riemann methods provide an effective tool for solving the shallow flow equations numerically and predicting unsteady motion of debris flows and flash floods along paths with arbitrary geometry and inclination.

INTRODUCTION

Debris flows are churning, water-saturated masses of fine sediment, rocks, and assorted detritus that originate on mountain slopes and course down stream channels when they reach valley floors. Strong interactions of solid and fluid forces greatly influence the behavior of debris flows and distinguish them from related phenomena such as rock avalanches and water floods (Iverson, 1997). However, flash floods can resemble debris flows if floods entrain enough woody debris or coarse sediment to markedly increase friction at the fronts of advancing bores.

Mechanistic modeling of debris flows and debris-laden flash floods traditionally entails fitting model predictions to field data by adjusting the values of flow-resistance coefficients. Uncertainties about flow rheology and resistance afford great latitude for adjusting coefficient values until desirable fits are attained. However, coefficient adjustment lends little mechanical insight and provides no foundation for development of improved theoretical models.

In this paper we describe a depth-averaged flow model that avoids use of adjustable coefficients in most circumstances. The model was originally developed to simulate debris flows but is readily adaptable to simulation of debris-laden flash floods. For debris-flow simulations, flow resistance is computed from the following quantities: flow-path topography represented by gridded elevation data, sub-grid-scale bed topography (roughness) represented by a Coulomb friction angle, the internal Coulomb friction angle of the granular solids, the pore-pressure diffusivity of the solid-fluid mixture,

and the viscosity and volume fraction of the fluid phase. For flood calculations viscous fluid resistance must be replaced by an expression that accounts for hydrodynamic turbulence. In all cases the model accounts for the strong influence of cross-stream momentum fluxes on flow dynamics, because it computes motion of debris flows or debris-laden floods across three-dimensional terrain.

GOVERNING EQUATIONS

We first summarize the depth-averaged equations of motion we use to simulate debris flows. Elsewhere we provide detailed derivations of these equations (Iverson and Denlinger, 2000; Denlinger and Iverson, 2000). The equations express the laws of conservation of mass and linear momentum for concentrated mixtures of Coulomb granular solids and Newtonian viscous liquids without significant fluid turbulence. The equations are referenced to a local coordinate system that is fitted to the underlying topography (Figure 1). For each local coordinate system (i.e. each cell or facet of topography) the equations may be written compactly as

$$\frac{\partial \mathbf{U}}{\partial t} + \frac{\partial \mathbf{F}}{\partial x} + \frac{\partial \mathbf{G}}{\partial y} = \mathbf{S} \quad (1)$$

$$\mathbf{U} = \begin{bmatrix} h \\ h\bar{v}_x \\ h\bar{v}_y \end{bmatrix} \quad \mathbf{F} = \begin{bmatrix} h\bar{v}_x \\ h\bar{v}_x^2 + \frac{1}{2}hc^2 \\ h\bar{v}_x\bar{v}_y \end{bmatrix} \quad \mathbf{G} = \begin{bmatrix} h\bar{v}_y \\ h\bar{v}_y\bar{v}_x \\ h\bar{v}_y^2 + \frac{1}{2}hc^2 \end{bmatrix} \quad \mathbf{S} = \begin{bmatrix} 0 \\ S_x \\ S_y \end{bmatrix} \quad (2)$$

where

$$S_x = g_x h - \text{sgn}(\bar{v}_x)(1 - \lambda) \left(g_z + \bar{v}_x^2 \frac{\partial \theta_x}{\partial x} \right) h \tan \phi_{bed} - \frac{3\nu_f \mu}{\rho} \frac{\bar{v}_x}{h} + \frac{\nu_f \mu h}{\rho} \frac{\partial^2 \bar{v}_x}{\partial x^2} + \text{sgn} \left(\frac{\partial^2 \bar{v}_x}{\partial y^2} \right) h k_{act/pass} \frac{\partial}{\partial y} [g_z h (1 - \lambda)] \sin \phi_{int} + \frac{\nu_f \mu h}{\rho} \frac{\partial^2 \bar{v}_x}{\partial y^2} \quad (3)$$

$$S_y = g_y h - \text{sgn}(\bar{v}_y)(1 - \lambda) \left(g_z + \bar{v}_y^2 \frac{\partial \theta_y}{\partial y} \right) h \tan \phi_{bed} - \frac{3\nu_f \mu}{\rho} \frac{\bar{v}_y}{h} + \frac{\nu_f \mu h}{\rho} \frac{\partial^2 \bar{v}_y}{\partial y^2} + \text{sgn} \left(\frac{\partial^2 \bar{v}_y}{\partial x^2} \right) h k_{act/pass} \frac{\partial}{\partial x} [g_z h (1 - \lambda)] \sin \phi_{int} + \frac{\nu_f \mu h}{\rho} \frac{\partial^2 \bar{v}_y}{\partial x^2} \quad (4)$$

$$\lambda = \frac{p_{bed}}{\rho g_z h} \quad (5)$$

$$k_{act/pass} = 2 \frac{1 \mp [1 - \cos^2 \varphi_{int} (1 + \tan^2 \varphi_{bed})]^{1/2}}{\cos^2 \varphi_{int}} - 1 \quad (6)$$

$$c = \sqrt{[(1 - \lambda)k_{act/pass} + \lambda]g_z h} \quad (7)$$

In these equations the independent variables are time t and the space coordinates x and y . The dependent variables are the depth-averaged velocity components $\bar{v}_x(x,y,t)$ and $\bar{v}_y(x,y,t)$ and the flow depth $h(x,y,t)$ in the z direction, normal to the bed (Figure 1). The function sgn used in (3) and (4) designates the sign (+ or -) of its argument.

The basic parameters in the governing equations are the components of gravitational acceleration, g_x , g_y , and g_z ; the components of the local bed slope, θ_x and θ_y (measured in radians from the horizontal); the internal and basal friction angles of the solid grains, φ_{int} and φ_{bed} ; the viscosity and volume fraction of the intergranular fluid, μ and v_f ; and the bulk density of the grain-fluid mixture, ρ . These fundamental, measurable parameters are used to derive the other coefficients in (1)-(4), which are defined in (5)-(7). The coefficient λ represents the ratio of the basal pore-fluid pressure, p_{bed} , to the total basal normal stress, $\rho g_z h$. Values of λ vary as a function of x , y , and t and are obtained by computing p_{bed} using an advection-diffusion equation described below. The longitudinal stress coefficient $k_{act/pass}$ is derived from Coulomb failure theory and determines the magnitude of grain-contact normal stresses in the x - y plane (Iverson, 1997). Typically, values of $k_{act/pass}$ exceed 1 where flow locally converges ($k = k_{pass}$) but are less than 1 where flow locally diverges ($k = k_{act}$). As a result, depth-averaged longitudinal stresses in grain-fluid mixtures are more complicated than those in one-phase fluid flows. The coefficient c is the gravity-wave speed that determines the rate of longitudinal information propagation in the flow. The equation defining c is more complicated than the analogous equation for fluid flows, owing to the effects of longitudinal grain stresses and variable fluid pressure. However, the definition of c reduces to the standard shallow-water definition $c = \sqrt{g_z h}$ if the grain-fluid mixture is fully liquefied ($\lambda = 1$) and Coulomb grain-contact stresses vanish.

The most obvious difference between (1)-(4) and the conventional shallow-water equations exists in the source terms, S_x and S_y , which represent the sum of driving and resisting forces per unit area of the bed (divided by ρ). The equations defining S_x and S_y each contain six terms. In order, these terms have the following physical significance: 1. gravitational driving force; 2. resisting force due to granular Coulomb friction at the bed, which is influenced by bed curvature; 3. resisting force due to viscous fluid drag resolved at the bed; 4. longitudinal normal force due to viscous fluid elongation or compression in the direction of flow; 5. intergranular Coulomb force due to velocity gradients transverse to the direction of flow; and 6. viscous fluid force due to velocity gradients transverse to the direction of flow. Forces associated with longitudinal stress gradients due to variations in h are excluded from S_x and S_y and instead are contained within c , as noted above.

In S_x and S_y the terms involving space derivatives of bed slope account for all effects of bed curvature (e.g., $\partial\theta_x/\partial x = 1/r_x$, where r_x is the x component of the local radius of curvature; Figure 1). These curvature terms represent the effects of coordinate transformations that show how changes in bed slope redirect x and y momentum components to keep them parallel to the bed (e.g., Savage and Hutter, 1991). Redirection of the x and y momentum components influences basal normal stresses and thereby produces changes in Coulomb resistance and flow thickness. Where finite changes in bed slope occur between adjacent computational cells, we use the approximation $\partial\theta_x/\partial x \approx \tan(\Delta\theta_x/\Delta x)$ to account for curvature of the bed (Denlinger and Iverson, 2000).

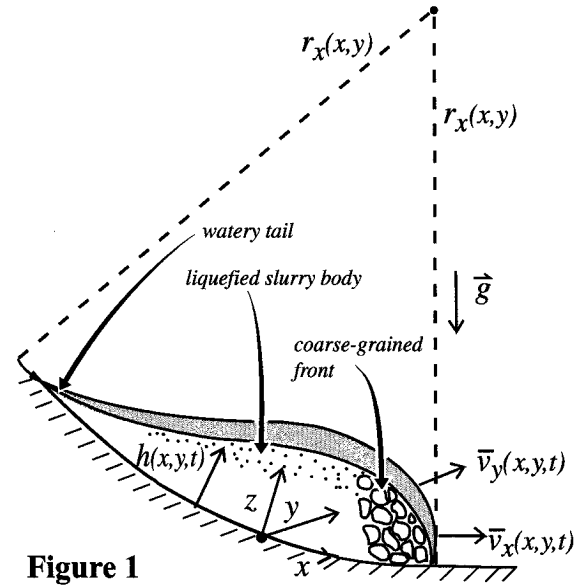


Figure 1

Evaluation of λ : The basal fluid-pressure ratio $\lambda = p_{bed}/\rho g_z h$ defined in (5) must be evaluated simultaneously with the dependent variables that describe flow, $\bar{v}_x(x,y,t)$, $\bar{v}_y(x,y,t)$ and $h(x,y,t)$. Guided by observations and measurements in large-scale experiments (Iverson, 1997; Major and Iverson, 1999), we infer that basal fluid pressures advect with depth-averaged flow and simultaneously diffuse normal to the bed, obeying (Iverson and Denlinger, 2000)

$$\frac{\partial p_{bed}}{\partial t} + \bar{v}_x \frac{\partial p_{bed}}{\partial x} + \bar{v}_y \frac{\partial p_{bed}}{\partial y} = D \frac{\partial^2 p}{\partial z^2} \Big|_{bed} \quad (8)$$

where $|_{bed}$ designates that the diffusion term is evaluated at the bed, where $z = 0$. The pore-pressure diffusivity, D , determines the rate of pressure diffusion and is defined by $D = kE/\mu$, where k is the intrinsic hydraulic permeability of the aggregate solid debris and E is its compressive stiffness. For typical debris-flow mixtures D has values in the range 10^{-7} - 10^{-3} m²/s (Iverson, 1997; Major et al., 1997). These values imply, for example, that excess fluid pressures in flows 1 m thick can persist for times ranging from minutes to months, once excess pressures are established. (Excess fluid pressures are those in excess the hydrostatic fluid pressure, $p_{bed} = \rho_{fluid} g_z h$. This hydrostatic pressure is less than the total basal pressure $\rho g_z h$ used to define λ , because the fluid density ρ_{fluid} is less than the total mixture density, ρ .) Excess fluid pressures are generally established during the initial stages of debris-flow motion due to soil contraction and liquefaction (Iverson et al., 2000).

Modification for Flash Floods: Fluid forces play a different role in flash floods than in debris flows because volumetric sediment concentrations in the body of flash floods are too low to form an interconnected granular matrix. Therefore, in the body of flash floods, Coulomb grain-contact forces are negligible and pore-pressure diffusivity is irrelevant. Consequently, we infer that fluid pressures are uniformly hydrostatic (the usual shallow-water assumption) in the body of flash floods and that suspended solids merely increase the fluid density. We also infer that turbulent energy dissipation is important in flash floods, and that the viscous resistance terms in (3) and (4) must be replaced by

terms representing the effects of turbulence. Adopting turbulence terms suggested by Vreugdenhil (1994), we reduce (3)-(7) to forms applicable to the watery body of flash floods

$$S_x = g_x h - s_f \bar{v}_x \sqrt{\bar{v}_x^2 + \bar{v}_y^2} \quad (9)$$

$$S_y = g_y h - s_f \bar{v}_y \sqrt{\bar{v}_y^2 + \bar{v}_x^2} \quad (10)$$

$$\lambda = 1 \quad (11)$$

$$k_{act/pass} = 1 \quad (12)$$

$$c = \sqrt{g_z h} \quad (13)$$

These relationships demonstrate that the standard shallow-water equations are a special case of our debris-flow equations (modified to account for fluid turbulence).

The dimensionless turbulent stress coefficient s_f used in (9) and (10) depends on relative boundary roughness and Reynolds number, and its value cannot, in general, be specified without some estimate of flow speeds and depths. However, for flows on rough beds at high Reynolds numbers ($> 10^5$), values of s_f commonly are of the order of 0.1. For flows across rugged terrain, exact values of s_f are relatively unimportant because multidimensional momentum transport described by equations (1) and (2) accounts for the effect of topography on water-surface slopes (Denlinger et al., 1998).

If the leading margin of a flash flood scours or abrades stream banks or the bed and thereby acquires substantial quantities of woody debris or coarse sediment, the flood wave may act somewhat like a debris flow with a high-friction snout and low-resistance tail. To model the mechanics of a debris-laden bore, equations (9)-(13) can be blended with the more general equations (3)-(7). In this case values of the basal fluid-pressure ratio vary from $\lambda = 0$ at the leading edge of the bore, where solid Coulomb friction dominates resistance, to $\lambda = 1$ in the part of the flood where fluid turbulence dominates resistance. For flash floods, of course, energy dissipation due to fluid forces is modeled using the turbulent stress terms in (9) and (10) rather than the viscous stress terms in (3) and (4).

Discrimination of Bore Fronts: A key step in computing motion of debris flows and flash floods with debris-laden bores involves discrimination of bore-front regions with low values of λ and high Coulomb friction. Equation (8) with constant pore-pressure diffusivity is insufficient for this purpose. According to (8), the only factors affecting the distribution of λ are initial conditions, downstream pressure advection, and the local flow thickness and pore-pressure diffusivity. To these factors we add kinematic criteria for identifying fronts of bores, which we infer have elevated diffusivities and depleted pore pressures. We identify fronts of bores as those regions where flow thickness decreases in the downstream direction. Such regions satisfy one or more of the kinematic criteria

$$\begin{aligned}
\bar{v}_x > 0 \quad \text{and} \quad \partial h / \partial x < 0 \\
\bar{v}_x < 0 \quad \text{and} \quad \partial h / \partial x > 0 \\
\bar{v}_y > 0 \quad \text{and} \quad \partial h / \partial y < 0 \\
\bar{v}_y < 0 \quad \text{and} \quad \partial h / \partial y > 0
\end{aligned}
\tag{14}$$

Where such criteria are met, we increase D significantly (typically by 1-2 orders of magnitude) before solving (8). In the extreme case of a bore composed entirely of large rocks or woody debris, we assume that D is essentially infinite and that no fluid pressure can be sustained. This simplistic assumption yields relatively good predictions of debris-flow motion (Denlinger and Iverson, 2000).

Mass Change (Erosion and Sedimentation): Debris flows and debris-laden flash floods can significantly change their mass by entraining or depositing debris in transit, and mass change may significantly affect flow dynamics. Mass change is a three-dimensional process. Field observations indicate that flow mass typically increases as a result of undermining and scouring channel banks, and that flow mass decreases progressively where channels widen or slopes decline.

Mass-change terms can be added with little difficulty to the momentum and mass balances expressed in (1) and (2), but a significant difficulty attends use of such terms. Mass change depends on poorly constrained external forces that govern substrate strength and influence momentum transfer between the flowing mass and its three-dimensional boundaries (Iverson, 1997). These external forces must be included in models that compute adjustments of the basal boundary position due to erosion and sedimentation. For the present, we ignore the possibility of mass change and focus on the simpler case in which boundaries are fixed and flow mass is constant. Evaluation of forces associated with mass change remains an outstanding problem that must be solved to develop a complete understanding of the dynamics of debris flows and flash floods.

NUMERICAL SOLUTION TECHNIQUE

The nonlinear, hyperbolic partial differential equations (1)-(4) require special techniques for numerical solution in arbitrarily complex domains such as those imposed by three-dimensional flow-path topography. We use a technique that constructs solutions throughout complex flow domains by solving elementary Riemann problems that govern the magnitudes and directions of mass and momentum fluxes through the walls of individual computational cells (Toro, 1997). Elsewhere, we describe details of our technique (Denlinger and Iverson, 2000). Here we outline some aspects of the technique that are particularly important for computing motion of debris flows and flash floods.

The Riemann methodology recasts equations (1) and (2) in terms of Jacobian matrices \mathbf{A} and \mathbf{B} . Then (1) becomes

$$\frac{\partial \mathbf{U}}{\partial t} + \mathbf{A} \cdot \frac{\partial \mathbf{U}}{\partial x} + \mathbf{B} \cdot \frac{\partial \mathbf{U}}{\partial y} = \mathbf{S}
\tag{15}$$

where

$$\mathbf{A} = \begin{bmatrix} 0 & 1 & 0 \\ c^2 - \bar{v}_x^2 & 2\bar{v}_x & 0 \\ -\bar{v}_x\bar{v}_y & \bar{v}_y & \bar{v}_x \end{bmatrix} \quad \mathbf{B} = \begin{bmatrix} 0 & 0 & 1 \\ -\bar{v}_x\bar{v}_y & \bar{v}_y & \bar{v}_x \\ c^2 - \bar{v}_y^2 & 0 & 2\bar{v}_y \end{bmatrix} \quad (16)$$

The Riemann problem consists of first computing the trajectories along which information about the conserved variables \mathbf{U} propagates in space and time (given by eigenvectors of \mathbf{A} and \mathbf{B}), and then balancing fluxes of the conserved variables along these trajectories. Explicit Euler integration incorporates the effects of the source terms, \mathbf{S} , and advances the solution in time. This approach has great advantages for minimizing numerical dispersion and tracking shocks. Accurate shock tracking is more important for predicting behavior of debris flows and flash floods than is typically the case for slower water floods. Prevalence of steep flow paths, abrupt flow fronts, severe topographic obstructions, and variability of the gravity-wave speed, c , commonly causes shock-rich behavior in debris flows and flash floods.

Numerous techniques have been devised for numerical solution of Riemann problems (Toro 1997). Techniques differ chiefly according to the scheme used to balance fluxes across grid-cell boundaries. We use a technique (called HLLC) that generates approximate solutions to exact Riemann problems involving the nonlinear terms in \mathbf{A} and \mathbf{B} (Toro, 1997). Denlinger and Iverson (2000) provide details of our implementation of the HLLC solver.

Flow-front Propagation Speeds: Debris flows and flash floods have sharply defined flow fronts, which pose unique challenges for predictive models. Numerically, such fronts occur wherever zero flow depth exists adjacent to a computational cell. Our means of computing the speeds of these fronts follows a rationale like that of Toro (1997, p. 140) for an analogous problem involving vacuum fronts in shock tubes. Here we focus on the equation governing the speed of a flow front advancing in the right-hand (positive x) direction, but analogous equations apply to advancing and receding fronts in all directions.

Mass and momentum conservation dictate that physical information emanating from flow fronts propagates in a manner that preserves a quantity (known as a Riemann invariant) defined by

$$I_L = \bar{v}_x|_L + 2c_L \quad (17)$$

for the case $S_x = 0$. Here the subscript L denotes waves moving left (upstream) from the flow front. Very near the flow front (where $h \rightarrow 0$ and $v_f \rightarrow 0$), it is reasonable to assume that $S_x \rightarrow 0$, and we therefore assume that I_L is approximated well by (17). We then equate values of I_L at the flow front (denoted by subscript 0) and at any other point just upstream of the flow front, yielding

$$\bar{v}_x|_0 + 2c_0 = \bar{v}_x|_L + 2c_L \quad (18)$$

However, near the flow front the gravity wave speed c approaches zero because $h \rightarrow 0$, and precisely at the front, $c_0 = 0$ exactly. Substituting this value in (18) and combining the result with (17) yields

$$\bar{v}_x|_0 = I_L \quad (19)$$

which indicates that the speed of the mixture at the flow front equals the Riemann invariant associated with the left-going waves emanating from the flow front. Moreover, since the mixture thickness tapers to zero at the flow front, the mixture speed equals the speed of the front itself. Effectively, the speed of the right-going front is dictated by the rate at which material discharges from the left.

CONCLUDING DISCUSSION

This paper highlights key features of a mathematical model we have developed to simulate motion of debris flows and debris-laden flash floods. Elsewhere, we describe details of model formulation and tests of model predictions against experimental data for dry granular avalanches and water-saturated debris flows (Iverson and Denlinger, 2000; Denlinger and Iverson, 2000). Here we introduce model modifications necessary to simulate motion of debris-laden flash floods. In all cases a central feature of the model is use of depth-averaged mass- and momentum-conservation equations applicable to flow over three-dimensional terrain. Another key feature is use of a Riemann solution algorithm that does not restrict model applications to smooth or gently sloping beds. These features appear crucial for extending the model to analyze flows that change mass as they move through realistic landscapes.

REFERENCES

- Denlinger, R.P., Walters, R.A., Ostenaar, D., Levish, D., 1998, Robust methods for routing floods over highly irregular terrain, *Proceedings of the First Federal Interagency Conference on Floods*, Las Vegas, Nevada, April, 1998. 6-89 - 6-95.
- Denlinger, R.P., Iverson, R.M., 2000, Flow of variably fluidized granular masses across 3-D terrain: 2. Model predictions and experimental tests, *Journal of Geophysical Research (B)*, in press.
- Iverson, R.M., 1997, The physics of debris flows, *Reviews of Geophysics*, 35, 245-296.
- Iverson, R.M., Denlinger, R.P., 2000, Flow of variably fluidized granular masses across 3-D terrain: 1. Coulomb mixture theory, *Journal of Geophysical Research (B)*, in press
- Iverson, R.M., Reid, M.E., Iverson, N.R., LaHusen, R.G., Logan, M., Mann, J.E., Brien, D.L., 2000, Acute sensitivity of landslide rates to initial soil porosity, *Science*, in press.
- Major, J.J., Iverson, R.M., 1999, Debris-flow deposition: effects of pore-fluid pressure and friction concentrated at flow margins, *Geological Society of America Bulletin*, 111, 1424-1434.
- Major, J.J., Iverson, R.M., McTigue, D.F., Macias, S., and Fiedorowicz, B.K., 1997, Geotechnical properties of debris-flow sediments and slurries, in *Debris-flow Hazards Mitigation: Mechanics, Prediction, and Assessment*, C.L. Chen, ed., American Society of Civil Engineers, 249-259.
- Savage, S.B., Hutter, K., 1991, The dynamics of avalanches of granular materials from initiation to runout, Part I. analysis, *Acta Mechanica*, 86, 201-223.
- Toro, E.F., 1997, *Riemann Solvers and Numerical Methods for Fluid Dynamics*, Springer-Verlag, 492 p.
- Vreugdenhil, C.B., 1994, *Numerical Methods for Shallow-water Flow*, Kluwer, 261 p.